

Network, cluster coordinates and $N = 2$ theory II: Irregular singularity

Dan Xie

*School of Natural Sciences, Institute for Advanced Study
Princeton, NJ 08540, USA*

ABSTRACT: Cluster coordinates for a large class of Argyres-Douglas and asymptotical free theories are constructed using network on bordered Riemann surface. Such $\mathcal{N} = 2$ theories are engineered using six dimensional $(2, 0)$ theory on Riemann surface with irregular and regular singularities. The Stokes phenomenon plays an important role in our construction. Our results are expected to be very useful in studying BPS spectrum, wall crossing, and line operators of these theories, etc. In particular, we conjecture that the quiver from the network is the BPS quiver. Moreover, our construction provides a simple way to build the minimal network for cells of positive Grassmannia .

Contents

1. Introduction	1
2. Review	3
2.1 UV and IR data of AD theory	3
2.2 Dot diagram, network and quiver	5
2.3 Quiver and mutation	6
3. Stokes phenomenon	7
3.1 Integer pole	8
3.2 Type I irregular singularity	12
3.3 Type II irregular singularity	13
4. Cluster coordinates for Argyres-Douglas theory	15
4.1 Type I AD theory	16
4.1.1 (A_1, A_{N-1}) theory	16
4.1.2 (A_{k-1}, A_{nk-1}) theory	17
4.1.3 Generic case	20
4.2 Type II AD theory	23
4.3 Type III AD theory	25
4.4 Type IV AD theory	26
5. Cluster coordinates for asymptotical free theory	28
5.1 Linear quiver with Lagrangian descriptions	28
5.1.1 One gauge group	28
5.1.2 Linear quiver	30
5.2 Theory with AD matter	31
6. Conclusion	33

1. Introduction

A large class of four dimensional $\mathcal{N} = 2$ Argyres-Douglas theory (AD) [1, 2] can be engineered from six dimensional $A_{k-1} (2, 0)$ theory using the irregular singularity [3]. Instead of specifying the UV Lagrangian theory and studying the scaling limit to find AD theory, our construction is much more simpler by just describing the form of the irregular singularity. Such construction is very powerful in answering many physical questions: all the dimensional coupling constants and the number of mass parameters can be read directly

from the form of irregular singularity; the scaling dimensions of chiral primary operators of the theory can be easily listed; the Seiberg-Witten curve and three dimensional mirrors can be written down pretty easily; the central charges can be quickly calculated; these AD theories can be used nicely in forming new asymptotical free theories which also have six dimensional constructions, etc.

Many other dynamical properties of these theories can be found from this magical geometric construction: the BPS spectrum and wall crossing behavior, the classification of line operators and its expectation value could be extracted from the combinatoric object defined on the Riemann surface. The moduli space \mathcal{M} of Hitchin equation with irregular singularity plays a central role here. \mathcal{M} is the Coulomb branch of the four dimensional theory compactified on a circle and is a Hyperkahler manifold [4]. A special coordinate system called cluster coordinates [5] on framed ¹ version of \mathcal{M} seems to be really important in studying these properties as the study in $SU(2)$ case indicated:

1. Finding the BPS spectrum and studying the wall crossing behavior of a 4d $\mathcal{N} = 2$ theory [6, 7, 8, 9, 10].
2. The classification of the line operators [11], the BPS wall crossing in the presence of line defects and surface defects [12, 13].

Given the importance of the cluster coordinates, it would be really interesting to find such coordinates for the AD theory and asymptotical free theory constructed in [3]. The purpose of this paper is to achieve this goal. The essential definition of the cluster coordinates involves a quiver, or more precisely a quiver mutation class. We are going to find quiver mutation class for these $\mathcal{N} = 2$ theories using simple combinatorial methods.

\mathcal{M} in one of complex structure describes the flat connections with irregular singularity [4, 14]. The solutions of the flat section equation have the very interesting Stokes phenomenon and the moduli space can be defined using Stokes matrices. Basically, Stokes phenomenon captures how the asymptotical behavior of the solutions changes in different angular region around the singularity. The Stokes matrix is actually a unipotent subgroup and one could use a Young Tableaux to label it, this is the most important starting point for our construction. We blow up the irregular singularity into a disc and put a marked point with a Young Tableaux label for each Stokes matrix. Given such a cyclic ordering of the Young Tableaux, the method proposed in [15] can be used to construct a dot diagram and a bipartite network from which a quiver can be read.

The detailed procedure for finding the quiver is the following: Start with a triangulation of the disc with labeled marked points, and decorate the internal and external edges using black and white dots based on the information of the punctures. Such decoration is uniquely fixed by the Young Tableaux and the triangulation. Each triangle is further tessellated using two types of minimal polygons and then a bipartite network could be found from the dot diagram. One only need to know the quiver for the triangle and the whole quiver is derived by gluing the quivers of the triangles together.

The first use of the quiver is to confirm some of the isomorphism proposed in [3]. The same theory can be realized by using different A_N theory and different singularity

¹Framed can be thought of adding some extra parameters to the moduli space.

combinations, we show that different configurations give the quiver in the same mutation class. Our result agrees with what is found in the literature for those theories whose BPS quiver is known in some form. Our construction is very simple and purely combinatorial, moreover, our result has another virtue: the quiver mutation sequences which leads back to the original quiver can be easily found, such sequences are very important in finding the BPS spectrum and studying the wall crossing behavior. This result has great meaning since generically the quiver studied in this paper is in a mutation infinite class, it is very hard to find the above sequences if we do random quiver mutations. Moreover, our quiver and the cluster coordinates are actually describing a very interesting moduli space.

This paper is organized as follows: Section 2 review the basic data for the irregular singularity and regular singularity relevant for the AD theory constructed in [3], we also review how to find the quiver based on a cyclic ordering of Young Tableaux. Section 3 describes the Stokes phenomenon and the Young Tableaux label for the irregular singularity. Section 4 is a detailed discussion on how to find the quivers for the AD theory, many examples are given. Section 5 discusses the construction of the quiver for non-conformal theory. Finally, we give a short discussion on the possible applications of our result in section 6.

2. Review

2.1 UV and IR data of AD theory

A large class of four dimensional SCFTs can be engineered by compactifying six dimensional A_{k-1} $(2,0)$ theory on a punctured Riemann surface. The theory of class \mathcal{S} [16, 7] is engineered by putting arbitrary number of regular singularities (first order pole) on a Riemann surface. Theory \mathcal{S} has integer scaling dimensions and have dimensionless gauge coupling constants. On the other hand, the Argyres-Douglas (AD) theory has dimensional coupling constant and irregular singularity (higher order pole) is needed. Moreover, there are two constraints on the choice of the Riemann surface and the combination of the singularities: first, only Riemann sphere can be used; second, only one irregular singularity or one irregular singularity and one regular singularity at opposite poles are viable.

The regular singularities are classified by Young Tableaux which specifies a partition $k = n_1 + n_2 + \dots + n_r$. We use the notation $Y = [n_1, n_2, \dots, n_r]$ to denote the Young Tableaux. There are $r-1$ mass parameters encoded in this puncture and the corresponding flavor symmetry could also be read from Y . There are two special punctures which we want to give them special name: The full puncture has partition $[1, 1, \dots, 1]$ whose flavor symmetry is $SU(k)$; The simple puncture has the partition $[k-1, 1]$ and the flavor symmetry is $U(1)$.

The irregular singularity useful for the AD theory are much more fruitful and a complete classification is given in [15]:

a. Type I singularity: the holomorphic part of the Higgs field ²

$$\Phi = \frac{1}{z^{n+j/k+2}} \text{diag}(1, \omega, \omega^2, \dots, \omega^{k-1}) \quad (2.1)$$

with $\omega = \exp(\frac{2\pi i}{k})$ and z a local coordinate on Riemann sphere. Here $n \geq -1$ is an integer and $0 \leq j < k$. All the subleading terms compatible with the leading order form are allowed ³. The AD theory for this class of irregular singularities are first studied in [17].

b. Type II singularity: the Higgs field has the form

$$\Phi = \frac{1}{z^{n+j/(k-1)+2}} \text{diag}(0, 1, \omega, \omega^2, \dots, \omega^{k-2}) \quad (2.2)$$

with $\omega = \exp(\frac{2\pi i}{k-1})$ and $0 < j < k-1$. We ignore the subleading terms compatible with the leading order behavior. Several lower rank examples of this class are discussed in [18, 19].

c. Type III singularity: The leading order pole is integer but the coefficient is not regular semi-simple. The classification is given by a sequence of Young Tableaux such that $Y_n \subset Y_{n-1} \subset \dots \subset Y_1$.

The first and second irregular singularity are nicely reflected geometrically by a Newton polygon: Starts with the unit two dimensional lattice and label the horizontal coordinate as z and the vertical coordinate as x ⁴. The Newton polygon is formed by a sequence of lines ending on lattice points in the region ($x \geq 0, z \geq 0$).

The slop of type I singularity is $r = n + j/k$, while the slops of two edges of type II singularities are $r = n + j/(k-1)$ and $r = n$ respectively. Many information of the four dimensional SCFT can be read from the corresponding Newton polygon, i.e. and the number of mass parameters are the number of integer points on the newton polygon.

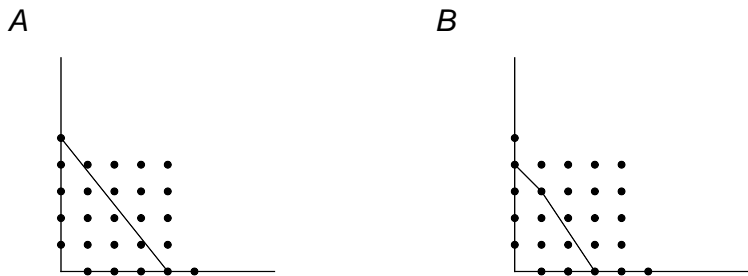


Figure 1: The Newton polygon for type I and type II irregular singularity.

The IR physics are described by the moduli space of Hitchin's equation with above specified boundary conditions. In particular, the Seiberg-Witten curve is identified with the spectral curve of the Hitchin system. In the case of AD theory, one can easily find the full

²The Higgs field is a one form field defined on the Riemann surface, and there is also a gauge field appearing in Hitchin's equation. The Hitchin's moduli space is defined as the space of the solutions with the specified boundary condition on these fields.

³A gauge transformation is needed to make the solution consistent around the singularity, we require the subleading singular terms should also be consistent with this gauge transformation, i.e. they are going back to themselves after circling around the singularity followed by the gauge transformation.

⁴ x is the coordinate on cotangent bundle.

Seiberg-Witten curve from the corresponding Newton polygon of the irregular singularity,, i.e. the monomials appearing in Seiberg-Witten curve is determined by the non-negative integer lattice points bounded by the Newton polygon. More details can be found in [3].

The AD theory constructed in this way include almost all the AD theories found in the literature, and we have a huge number of new examples. Moreover, the theory defined using regular singularities on the sphere can all be realized using the irregular singularity.

2.2 Dot diagram, network and quiver

The result in [15] is crucial for our construction of quivers. This subsection serves as a light review of the relevant construction. Given a triangle labeled by three Young Tableaux, one could find a dot diagram and a further tessellation of the triangle using the brane construction proposed in [20]. The three vertices of the triangle have coordinates $(N, 0), (0, 0), (0, N)$ in a two dimensional lattice with unit spacing. The dot diagram is found as follows:

- a. Decorate the boundary of the triangle using the information of the puncture, the white dots is used to represent the boxes on the same column of the Young Tableaux.
- b. Construct the dot diagram inside the triangle using only following two types of polygons whose edge is formed by lines ⁵ connecting two black dots. 1: Triangles whose edges have the same length. 2: Trapeziums whose parallel sides have lengths n_1, n_2 and the other two sides have length $n_1 - n_2$ ⁶.

To state our rules for constructing the bipartite network ⁷, we need to distinguish two types of polygons in the tessellation of the big triangle: The type A polygon is the one whose triangle completion has the same orientation as the big triangle, and the triangle completion of the type B polygon has opposite orientation. The colored vertices in each polygon of the tessellation are determined in the following way (see figure. 2):

- a: Assign a white vertex to each type A polygon.
- b: Assign a black vertex to each type B polygon.

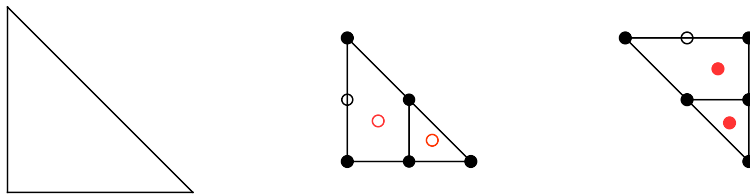


Figure 2: Left: The orientation of the big triangle. Middle: Put a white vertex to each polygon whose triangle completion has the same orientation as the big triangle. Right: Put a black vertex to each polygon whose triangle completion has opposite orientation.

A network is formed by connecting the white vertex and black vertex if there is a common edge between two corresponding polygons. We never connect two vertices with same color even if the corresponding polygons have one common edge. Finally, there is

⁵The lines should be parallel with the boundary edges.

⁶This constraint is from the supersymmetric condition on the brane configuration.

⁷A bipartite network has vertices colored with the black or white, and there are no edges connecting the vertices with the same color.

one line coming out of boundary for the vertex inside the polygon which has one piece of boundary edge of the triangle. The network formed in this way is always bipartite but there may be vertices with only two edges. We can use various moves to remove these degree-2 vertices and get another bipartite network from which a quiver without two cycles can be read in the following two steps:

Step1: Remove degree two vertices and then use the contraction to form another bipartite graph.

Step 2: Assign a quiver node to each surface and the quiver arrows are determined by the black vertices: there is a clockwise closed circles around it.

The three punctured network is a basic building block for more complicated cases. For more punctures, we start with a triangulation and decorate the internal edges which is derived by using the gauge theory result [21]. After these decorations on the edges of the triangulation, we can do the tessellations on each triangle and find the network, quiver, etc. Different triangulations are related by the a sequence of so-called flip which relate two triangulations of the quadrilateral, we have proved that if the dot diagram on all the punctures does not have the "bad" configuration shown in figure. 3, the corresponding quivers are related by quiver mutation (more precisely the two networks are related by square moves). However, if we consider only the quiver nodes represented by the closed surfaces, even with the "bad" corner, the quivers from different triangulations can still be isomorphic as we show later.

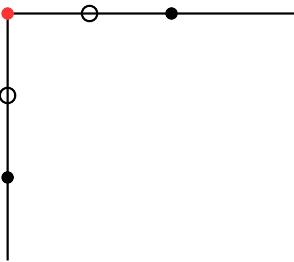


Figure 3: The network would be non-minimal if the boundary of the dot diagram has this form at any vertex.

The planar network has been studied in greater detail in describing the cells of the positive Grassmannia in [22]. Our result in this paper will give some simple ways of constructing minimal network. The higher rank generalization of the cluster coordinates for boarded Riemann surface is given in a seminal paper by Fock and Goncharov [23], and the similar network construction is also recently considered by Goncharov [24].

2.3 Quiver and mutation

A quiver is a directed graph where multiple arrows between two vertices are allowed. The quiver mutation for a quiver without one and two cycles is defined as the following: Let Q be a quiver and k a vertex of Q . The mutation $\mu_k(Q)$ is the quiver obtained from Q as follows, see figure. 4:

- 1) for each sub quiver $i \rightarrow k \rightarrow j$, create a new arrow between ij starting from i ;

- 2) we reverse all arrows with source or target k ;
- 3) we remove the arrows in a maximal set of pairwise disjoint 2-cycles.

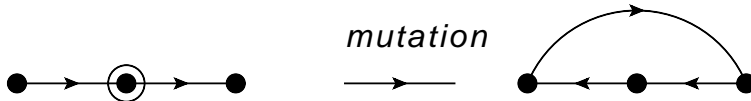


Figure 4: The quiver mutation.

Geometrically, a quiver could be found from the triangulation of the boarded Riemann surface and the quiver mutation is realized as the flip on the triangulation. The quiver can also be found from a bipartite network using the rule stated in last subsection and the quiver mutation is represented perfectly by the square move, see figure. 5. One can check the two quivers are related by quiver mutation. Notice that the above two geometrical quiver mutations are special since the node under mutation always has four quiver arrows on it.

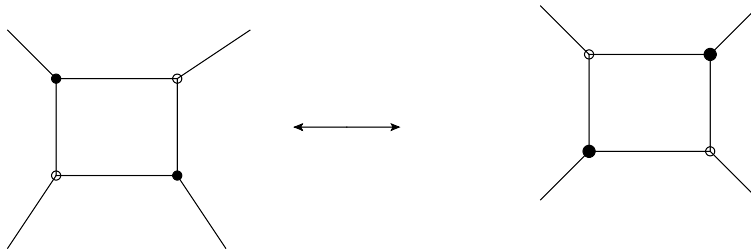


Figure 5: The square move which represents the quiver mutation.

Quiver mutation class of a quiver is defined as a collection of all the quivers which could be got by doing quiver mutation on it. Quiver with finite mutation class is the one with only finite number of quivers in this class. Most of the finite mutation class are associated with the triangulated surface of A_1 theory [25]. The ADE quiver is kind of special since the corresponding cluster coordinates are also finite. A type and D type quivers can be found from the triangulated surface. In this paper, we are going to show that the E type quiver can also be found from the triangulated surface but with A_2 group.

Quivers are used to study the BPS spectrum of $\mathcal{N} = 2$ theory and the corresponding $\mathcal{N} = 2$ theory for finite quiver mutation classes are found in [8]. One of the motivation of this paper is to find the quiver for other $N = 2$ theory related to general Argyres-Douglas theory discussed in [3], and most of the quivers discovered in this paper are mutation infinite.

3. Stokes phenomenon

The Coulomb branch of four dimensional field theory compactified on a circle is described by the Hitchin's moduli space with irregular singularity. The purpose of this paper is to find the cluster coordinates for it. In one of the complex structure of the Hitchin's moduli space, each point describes a complex flat connection with irregular singularity.

The solution of the flat section equation with such singularity has very interesting Stokes phenomenon, namely, the asymptotical behavior of the solutions are different in different angular region, and the Stokes matrix is used to link the solutions in different regions. Those Stokes matrices define the generalized monodromy which is essential in describing the moduli space. The Stokes matrix is a unipotent group which are naturally labeled by a Young Tableaux, and the generalized monodromy data can be described by a disc with several marked points labeled by Young Tableaux, this is exactly the setup we need to apply the construction found in [15].

3.1 Integer pole

We would like to first discuss the Hitchin equation with irregular singularity in some more detail. Let's take a complex structure on the Riemann surface, the Hitchin equation reads

$$\begin{aligned} F - \phi \wedge \phi &= 0, \\ D\phi &= D * \phi = 0, \end{aligned} \tag{3.1}$$

where A is the connection and ϕ is a one form called Higgs field [26, 27]. By writing $\mathcal{A} = A + i\phi$, the Hitchin equation implies that the curvature of \mathcal{A} is flat. In fact, one can introduce a spectral parameter and define a family of flat connections.

The monodromy around the singularity can be calculated by solving the following flat section equation:

$$(\partial_z + \mathcal{A}_z)\psi = 0, \tag{3.2}$$

with \mathcal{A}_z the holomorphic part of the complex connection. Locally the above equation is just a first order differential equation defined on the disk.

Let's now turn to irregular singular solution to Hitchin's equation [14]. The simplest one with gauge group $SU(k)$ is

$$\begin{aligned} \phi &= \frac{u_n}{z^n} + \dots + \frac{u_2}{z^2} + \frac{u_1}{z} + c.c \\ A &= \alpha d\theta. \end{aligned} \tag{3.3}$$

Here we choose local coordinate $z = re^{i\theta}$, u_1, \dots, u_n are all diagonal matrices after using gauge symmetry, and they are regular semi-simple which means the eigenvalues are all different. We ignore the regular terms in the solution but one should keep in mind that they are always there. The abelianization of the singular terms is crucial for finding the irregular singular solution. This type of irregular singularity is the type I singularity with integer pole we reviewed earlier.

There is an interesting Stokes phenomenon for the differential equation (3.2) which is important to define the monodromy around the irregular singularity. We will review some aspects for the Stokes phenomenon for the completeness, the interested reader can find more details in [14, 28]. The appearance of these Stokes matrices are coming from the asymptotical behavior of the solutions to the equation $(\partial + \mathcal{A}_z)\psi = 0$. Assume the gauge group is $U(1)$, then the differential equation becomes

$$\frac{d\psi}{dz} = -\left(\frac{q_n}{z^n} + \frac{q_{n-1}}{z^{n-1}} \dots + \frac{q_1}{z} + B(z)\right)\psi, \tag{3.4}$$

here $B(z)$ is a holomorphic function which is regular at $z = 0$. The solution is very simple:

$$\psi = c(z) \exp Q(z),$$

$$Q(z) = \frac{q_n}{(n-1)z^{n-1}} + \frac{q_{n-1}}{(n-2)z^{n-2}} \dots + q_1(-\ln z), \quad (3.5)$$

$c(z)$ is a formal power series which is not convergent around the singularity. This solution can be used to build the solutions for the higher rank group: one have a vector of above solution with index $i = 1, 2, \dots, k$. However, the entries of solution vector have different asymptotical behaviors along different path to the singularity because

$$\left| \frac{\exp Q^i(z)}{\exp Q^j(z)} \right| \rightarrow \left| \exp\left(\frac{q_n^i - q_n^j}{(n-1)z^{n-1}}\right) \right|, \quad z \rightarrow 0. \quad (3.6)$$

The asymptotical behavior depends on the sign of $Re\left(\frac{q_n^i - q_n^j}{(n-1)z^{n-1}}\right)$, which are different in different angular regions. A Stokes ray of type (ij) is a ray in complex plane where $\frac{q_n^i - q_n^j}{z^{n-1}}$ takes the value in negative imaginary axis:

$$\theta(n-1) = \theta_0 + \pi p, \quad (3.7)$$

here $\theta_0 = \arg(q_n^i - q_n^j) + \frac{\pi}{2}$ and n is an integer; We also take $0 \leq \theta \leq 2\pi$. Let's discuss some aspects of Stokes rays' distribution. The angular width between two Stokes rays is

$$\Delta\theta = \frac{\pi}{n-1}. \quad (3.8)$$

There are a total of $2(n-1)$ Stokes ray for any pair of solutions. Similarly for any angular regions with width $\frac{\pi}{n-1}$, there is a Stokes ray for any pair with the form (ij) and $i > j$, so there are a total of $\frac{k(k-1)}{2}$ Stokes rays in this region which are called Stokes sector.

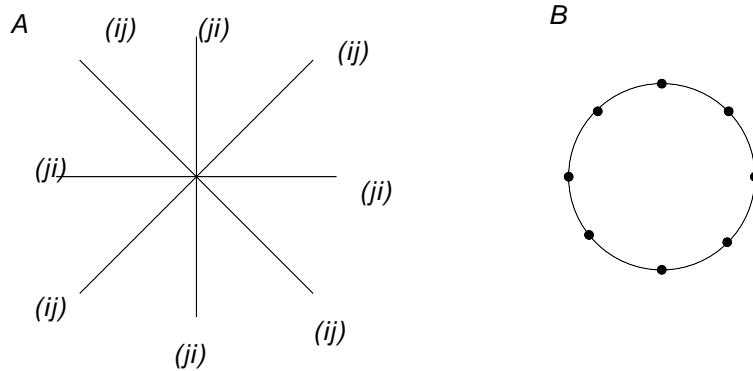


Figure 6: A: The Stokes rays for a pair of solutions to meromorphic differential equation on the disc. B: The disc model for the Stokes data of the irregular singularity.

The point is that the solution with given asymptotical behavior in a region is not unique if there is no Stokes ray. For example, if $\left| \frac{\exp(Q^i(z))}{\exp(Q_j(z))} \right| \gg 0$ in this region, then the solution $\psi'_i(z) = \psi_i(z) + \lambda\psi_j(z)$ has the same asymptotical behavior as ψ_i . Such freedom is

not here if there is a Stokes ray in this angular region as the asymptotical behavior changes in going through the Stokes ray. Let's take a region with angular width $\pi/(n-1)$ whose boundary is not a Stokes ray. By rotating this region by integer value of $\frac{\pi}{n-1}$, we get a cover of the disk. One can enlarge each sector a little bit such that there are no Stokes ray in the overlapping region. There will be a Stokes ray for any given pair of entries in the solution vector in each sector and the whole solution is uniquely fixed with given asymptotical behaviors in that region. On the overlapping region, the two sets of solutions are related by an upper triangular matrix with unit diagonal entry. This matrix is called the Stokes matrix and has the form (by proper renaming the indexes)

$$M = 1 + \sum_{i < j} c_{ij} E_{ij}, \quad (3.9)$$

where c_{ij} is a complex number and E_{ij} is the matrix where the only nonzero entry is $E_{ij} = 1$. Explicitly, the Stokes matrix has the following form.

$$M = \begin{pmatrix} 1 & * & * & * \\ 0 & 1 & * & * \\ 0 & 0 & 1 & * \\ 0 & 0 & 0 & 1 \end{pmatrix}$$

Each Stokes matrix has a total number of parameters $\frac{k(k-1)}{2}$ which equals to the total number of Stokes rays. The generalized monodromy⁸ is calculated by multiplying $2(n-1)$ Stokes matrices together:

$$M = M_1 * M_2 \dots * M_{2(n-1)}. \quad (3.10)$$

The simple graphic description for the generalized monodromy which are very useful for our later purpose is to blow up the irregular singularity to a disc and put $2(n-1)$ marked points on the boundary, each marked point is labeled by a full Young Tableaux ($Y = [1, 1, \dots, 1]$). The reason we assign such a Young Tableaux is determined by the form of the Stokes matrix which is a unipotent subgroup of $SL(k, C)$.

Let's introduce a little bit group theory which will be useful for our later generalization. For a diagonal matrix α , one could define a parabolic subgroup \mathcal{P} which are spanned by elements ψ satisfying

$$[\alpha, \psi] = \lambda \psi, \quad \lambda \geq 0 \quad (3.11)$$

The unipotent radical is derived by using the condition $\lambda > 0$. Now let's take $\alpha = \text{diag}(y_1, y_2, \dots, y_k)$ such that $y_1 > y_2 > \dots > y_k$, then the unipotent radical has the exact same form as the Stokes matrix we just had above. In general, let's use the Young Tableaux to describe the degeneracy of the eigenvalues of α , i.e. if the Young Tableaux is $Y = [n_1, n_2, \dots, n_r]$, then there are n_i diagonal entries with same real value, and we

⁸The full monodromy also has a formal monodromy part coming from the regular singular term, and the Hitchin's moduli space with irregular singularity is defined by fixing those parameters determining the formal monodromy.

take the same monotonically increasing order for the eigenvalues, then the corresponding unipotent radical is

$$S = \begin{pmatrix} I_1 & * & * & * & \dots \\ 0 & I_2 & * & * & \dots \\ 0 & 0 & I_3 & * & \dots \\ 0 & 0 & 0 & I_4 & \dots \\ \cdot & \cdot & \cdot & \cdot & \dots \end{pmatrix}$$

where I_j is a unit matrix with dimension $n_j \times n_j$.

Now let's relax the condition u_n is regular semi-simple and the irregular singularity is classified by a sequence of Young Tableaux $Y_n \subseteq Y_{n-1} \subseteq \dots \subseteq Y_1$. This is the type III irregular singularity according to classification. Let's study the solution to the meromorphic differential equation with such an irregular singularity. If two solutions have the same order of z dependence and the difference of them is

$$\psi_i - \psi_j = \frac{a_{i,j}}{z^l} + \dots \quad (3.12)$$

Then the level l Stokes ray [29] is defined as the ray in complex plane such that $\frac{a_{i,j}}{z^l}$ takes imaginary values. It is not hard to see that there are a total of $2(l-1)$ Stokes ray for each level l pair. To get the Stokes matrix and the full monodromy, we study the Stokes sector and the corresponding unipotent matrix in linking the solutions of two adjacent sectors.

Let's first start with the level $n-1$ Stokes ray, there are $2(n-1)$ Stokes sector following the above analysis, with the only exception that the unipotent matrix has the generalized form S , and the Young Tableaux of this Stokes matrix is Y_n , the disc model for level l is shown in figure. 7

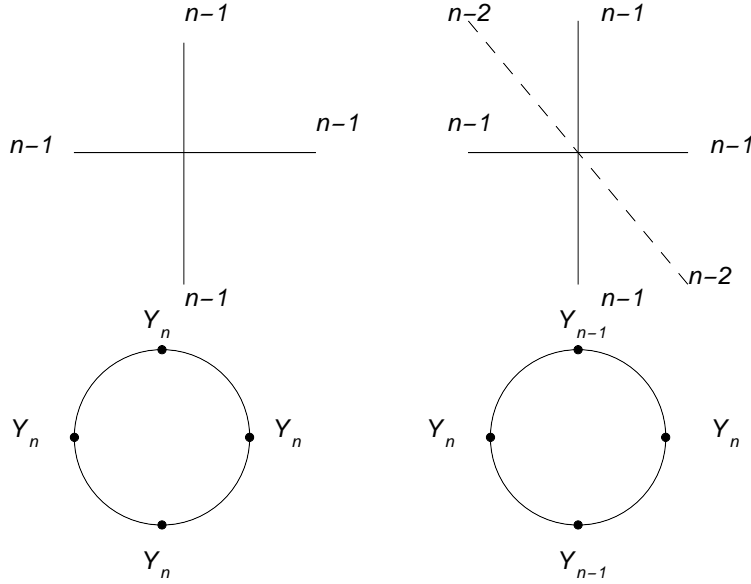


Figure 7: A: Stokes data for level $(n-1)$ Stokes rays. B: Level $(n-2)$ Stokes data.

If $Y_{n-1} \neq Y_n$, then some of the columns of Y_n is further partitioned, and we have level $(n-2)$ Stokes ray. However, the total number of Stokes sectors are only $2(n-2)$ for

this level. Now there are non-zero entries in the diagonal matrices I_{n_1} and the new Stokes matrix is determined by Y_{n-1} . However, there are only $2(n-2)$ matrices determined by Young tableaux Y_{n-1} , we are left with two Stokes matrices determined by Y_n . One can similarly label the generalized monodromy using the disc model with marked points on the boundary: there are a total of $2(n-1)$ marked points among which $2(n-2)$ have the label Y_{n-1} and 2 are labeled by Y_n . The cyclic order is that there are $(n-1)$ Y_{n-1} marked points followed by one Y_n marked points, and another $(n-1)$ Y_{n-1} followed by the last Y_n label.

One can generalize the above Stokes matrix analysis to other levels, the conclusion is that there are a total of $2(n-1)$ marked points on the boundary: for each Young Tableaux in the definition of the irregular singularity, there are two marked points sitting on the opposite sides of the line crossing the center of the circle. Moreover, the cyclic order of the Young Tableaux is exactly Y_n, Y_{n-1}, \dots, Y_2 on half circle, see figure. 8.

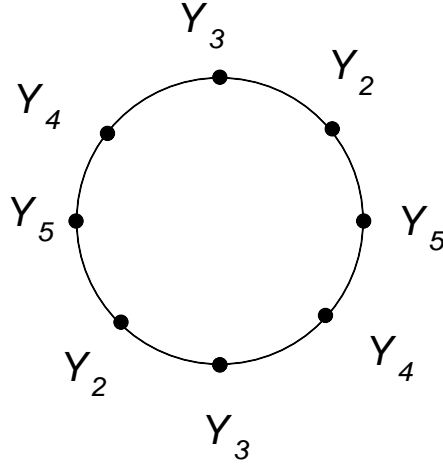


Figure 8: The stokes data for type III singularity.

A special note is that the dimension of the generalized monodromy is equal to the number of Stokes rays, which is equal to the total dimensions of all the Young Tableaux on the disc boundary if we use the dimension of the corresponding nilpotent orbit labeled by Y :

$$\dim(Y) = \frac{1}{2}(k^2 - \sum n_i^2). \quad (3.13)$$

For the full puncture, we have $\dim(Y) = \frac{1}{2}(k^2 - k)$ which is exactly the number of Stokes rays in a Stokes sector.

3.2 Type I irregular singularity

Let's recall the form of this type of irregular singularity which will appear in the definition of the meromorphic connection:

$$\Phi = \frac{1}{z^{n+j/k+2}} \text{diag}(1, \omega, \omega^2, \dots, \omega^{k-1}) + \dots \quad (3.14)$$

As we noted above, the key is to study the number of Stokes ray and its distribution. The Stokes phenomenon for this type of irregular singularity can be understood by going to the

covering space: let's define $z = t^k$, then the irregular singularity has the form

$$\Phi = \frac{1}{t^{(n+1)k+j+1}} \text{diag}(1, \omega, \omega^2, \dots, \omega^{k-1}) + .. \quad (3.15)$$

We ignore an overall real factor which is not important here. This irregular singularity is the familiar type where the leading order is regular semi-simple. The analysis of the Stokes phenomenon and Stokes matrices is now straightforward, however, one should note that not all the Stokes rays on the covering space are the actual Stokes ray on the original plane. Let's consider a pair of solutions corresponding to two eigenvalues of the irregular connection and assume the difference of them has the angular coordinate θ_0 , then the condition for the Stokes ray on the original space is

$$\theta_1(n + j/k + 1) = \theta_0 + \pi p \quad (3.16)$$

with p an integer and $0 \leq \theta_1 \leq 2\pi$. On the other hand, the condition for the Stokes ray on the covering space is

$$\theta_2((n + 1)k + j) = \theta_0 + \pi q \quad (3.17)$$

with q an integer and $0 \leq \theta_2 \leq 2\pi k$. So among k^2 Stokes rays in the covering space, only one is the real Stokes ray. Therefore the angular width of the Stokes sector is $\frac{\pi k^2}{(n+1)k+j}$. So we do not have an integer number of Stokes sector in the covering space.

What we are going to define the Stokes sector is the following: consider first $2(n + 1)$ maximal Stokes sector, and then $2j/k$ portion of the maximal Stokes sector which we call it S_0 . Since the Stokes rays are distributed equally in the covering space, we conclude that the total number of Stokes ray on this sector is

$$N_{S_0} = j(k - 1), \quad (3.18)$$

which can also be found by explicit calculations in the original space. Since the minimal unipotent group has dimension $(k - 1)$, and the fractional part of Stokes sector can be replaced by j simple Stokes matrices whose Young Tableaux is $[k - 1, 1]$.

The total number of Stokes rays are

$$N_{Stokes} = k(k - 1)(n + 1) + j(k - 1), \quad (3.19)$$

which is the total number of parameters for the generalized monodromy. The disc model for this type of irregular singularity is the following: one first have $2(n + 1)$ full punctures and then j simple punctures distributed on the disc in a cyclic order, see figure. 9. When k is even, and $j = \frac{k}{2}$, one could equivalently put $2n + 3$ full punctures on the boundary.

3.3 Type II irregular singularity

The Higgs field of this irregular singularity has the form

$$\Phi = \frac{1}{z^{n+j/(k-1)+2}} \text{diag}(0, 1, \omega, \omega^2, \dots, \omega^{k-2}) \quad (3.20)$$

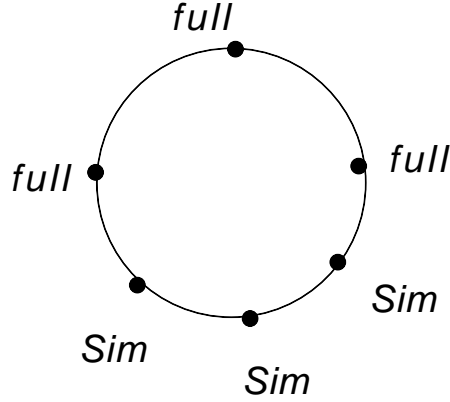


Figure 9: The Stokes data for type 1 singularity.

with $\omega = \exp(\frac{2\pi i}{k-1})$. The Stokes ray of a given pair of solutions is defined by the condition

$$\theta(n + 1 + j/(k - 1)) = \theta_0 + \pi p. \quad (3.21)$$

The angle difference between two Stokes rays is

$$\Delta\theta = \frac{\pi}{n + 1 + j/(k - 1)}. \quad (3.22)$$

The total number of Stokes rays are

$$N_{Stokes} = (n + 1)k(k - 1) + kj. \quad (3.23)$$

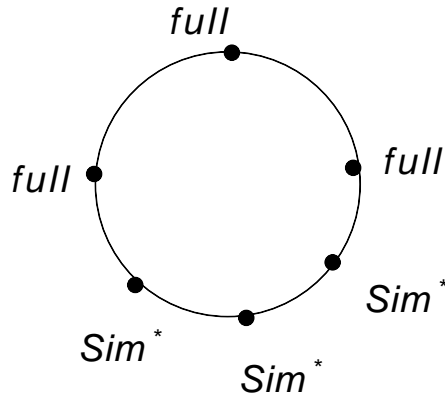


Figure 10: The disc model for type II singularity, here we need to include the boundary node from the simple puncture.

The difference with type I singularity is that there is an extra jk instead of $j(k - 1)$ number of Stokes rays. There is no simple representation using the Young Tableaux, but we have the following proposal: The disc model for such singularity is the same as the previous one, but we want to include the boundary nodes for the simple puncture, see figure. 10. This proposal will be confirmed in our later study, it would be interesting to prove it though. If k is odd, and $j = \frac{k-1}{2}$, one can put $(2n + 3)$ full punctures on the boundary to represent the monodromy data instead of gauging the boundary node.

4. Cluster coordinates for Argyres-Douglas theory

The generalized monodromy data for the irregular singularity is denoted by a sequence of Young Tableaux distributed on the boundary of the disc. The corresponding cluster coordinates are going to be constructed using the idea developed in [15]. In that paper, given a cyclic sequence of the Young Tableaux on the boundary, we can construct the network (equivalently quiver) from the ideal triangulation. We are going to show that the quiver actually has the same dimension as the rank of the charge lattice of the field theory, therefore, these coordinates are actually describing the moduli space of the framed local system in the presence of the irregular singularity. And we conjecture that the quiver is the corresponding BPS quiver.

This idea actually has firm grounding in the case when the irregular singularity has integer pole with leading order regular semi-simple. It is shown that the partial monodromy for a path around one vertex of the triangle [23] is actually upper-triangular which has exactly the same form as the Stokes matrix. It is interesting to verify that this fact is also true for the general punctures.

Let's discuss more about the ideal triangulation of Riemann surface with boundaries since the irregular singularity is replaced by a boundary with labeled marked points. Let us begin with a Riemann surface with boundaries, and specify a finite set of points M_{boundary} , called boundary marked points, on the boundary circles of Σ . Each connected component of $\partial\Sigma$ has at least one boundary marked point; The bulk puncture is not blown up and remained as a point in the interior of the Riemann surface. The defining data of our theory is a triple $(\Sigma, M_{\text{boundary}}, p)$, For notational convenience we sometimes denote this triple simply by Σ . In other words, Σ is defined by following data:

- a. the genus g of the Riemann surface;
- b. the number of bulk punctures p .
- d. the number b of boundary components;
- d. the number of marked points h_i on each boundary.

Each puncture represents the regular singularity while the boundary with marked points means an irregular singularity, all the marked points have a Young Tableaux label. The punctures and the marked points are all called marked points for simplicity in the following, and one should be careful about whether it is in the bulk or one the boundary. One can define a combinatorial object called ideal triangulation on above Riemann surface. An ideal triangulation is defined using arcs [25]. A simple arc γ in Σ is a curve such that

1. the endpoints of γ are marked points;
2. γ does not intersect itself, except at the endpoints;
3. γ is disjoint from the marked points and the boundary.

We also require the arc γ is not contractible into the marked points or onto the boundary. Each arc is considered up to isotopy. Two arcs are called compatible if they do not intersect in the interior of Σ . A maximal collection of distinct pairwise arcs is called an *ideal triangulation*. An edge is called external if it is isotopic to a segment of the boundary, otherwise it is called internal.

It is not hard to get the following formula for the number of internal edges:

$$6g + 3b + 3p + \# |M_{\text{boundary}}| - 6 , \quad (4.1)$$

where as defined previously g (b) is the genus (the number of boundary components) of Σ , respectively. The number of internal edges is $6g + 3b + 3p - 6$, and there are a total of $\# |M_{\text{boundary}}|$ external edges.

Once the ideal triangulation is given, one need to further tessellate the triangles to construct a dot diagram according to the marked points type, and then find the network and quiver. In this section, we will give a complete analysis of all the Argyres-Douglas constructed in [3], which involves at most one irregular singularity on the Riemann sphere, so we have only one boundary component. In the next section, we would consider general boarded Riemann surface which represents the asymptotical free theory.

4.1 Type I AD theory

4.1.1 (A_1, A_{N-1}) theory

Let's first study the construction of quiver for (A_1, A_{N-1}) theory using network (which is equivalent to the triangulation). The quiver for this theory is well known and our construction gives another combinatorial object: network which turns out to be very useful. The six dimensional construction involves a type I irregular singularity of A_1 group. The order of pole is $\lambda = \frac{N}{2} + 2$ so the number of marked points on the boundary is $n_{\text{marked}} = N + 2$ according to our previous analysis on Stokes data. The bordered Riemann surface is a disc with $(N + 2)$ marked points. There is only one type of puncture for A_1 theory, and all the marked points have the same type.

Example 1: The ideal triangulation of the disc with six marked points is given in figure. 11, which describes (A_1, A_3) theory. The network can be easily constructed and the quiver is also given in figure. 11 which is indeed of A_3 shape ⁹. Notice that the open surface on the boundary is not included as the quiver node, only the closed surface is used. Now we can do square moves and produce equally good coordinates, such square move is just a graphical representation of quiver mutation.

Let's give some general topological descriptions of the network. We add one external edge to the white vertices on the vertex of the triangulation and delete vertices with only two edges (which will not change the quiver). So there are a total of $N + 2$ external edges which is equal to the number of punctures. For a general network, define N as the total number of the punctures, then one can find an integer K from the following formula :

$$K - (N - K) = \sum \text{col}(v)(\text{deg}(v) - 2) , \quad (4.2)$$

where $\text{col}(v) = 1$ for black vertices and $\text{col}(v) = -1$ for white vertices. One could verify that k is not changed under quiver mutation and therefore this is a quiver mutation invariant. Each such network describes a positive cell in Grassmannia $G(N, K)$. It is easy to verify

⁹The orientation of the quiver arrows of this quiver is not important, since quivers with different orientations are related by quiver mutation.

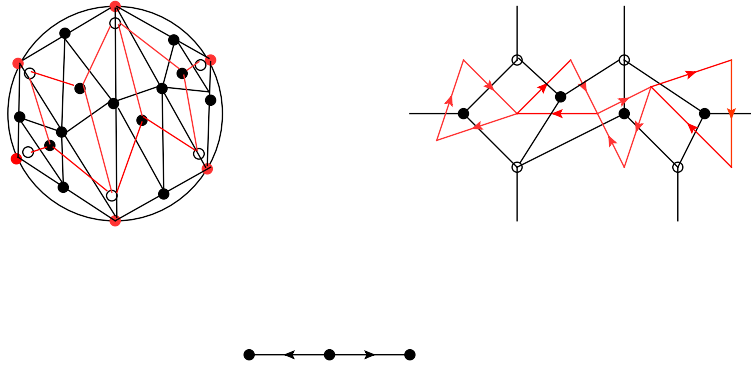


Figure 11: Left: the triangulation and the network for (A_1, A_3) theory. Right: The planar network and the quiver. Bottom: the quiver from the network and we keep only the nodes from the closed surface.

for (A_1, A_{N-1}) theory, K is always equal to 2, and the network describes maximal positive cell of $G(N+2, 2)$. Moreover, one could define the permutation using the zig-zag path which is also invariant under the square move.

4.1.2 (A_{k-1}, A_{nk-1}) theory

The next simplest case is the (A_{k-1}, A_{nk-1}) theory whose network can be found easily. The irregular singularity for this theory is

$$\Phi = \frac{A_r}{z^r} + \frac{A_{r-1}}{z^{r-1}} + \dots + \frac{A_1}{z}, \quad (4.3)$$

with $r = n+2$, and A_r, A_{r-1}, \dots, A_1 all have distinct eigenvalues. According to our previous analysis of the Stokes phenomenon, there are a total of $2(n+1)$ Stokes matrices arranged on the disk around the singularity. Each Stokes matrix is labeled by a full Young tableaux with partition $[1, 1, \dots, 1]$.

Geometrically, the Riemann sphere with irregular singularity is replaced by a disc with $(2n+2)$ marked points on the boundary. The triangulation of the disc has $(2n+2)$ external edges and $(2n-1)$ internal edges. The network is constructed from a triangulation and dot diagram on each triangle. The quiver is actually easy to find just from the dot diagram.

The total number of quiver nodes can be counted as following: the number is equal to the Coulomb branch dimension of the $\mathcal{N} = 2$ theory defined by putting the same number of full punctures on the sphere, which is equal to the sum of the dimension of all the Young tableaux minus the dimension of the gauge group

$$N = \frac{1}{2}2(n+1)(k^2 - k) - (k^2 - 1) = (k-1)(nk-1). \quad (4.4)$$

Amusingly, as shown in formula [6.21] of [3], the rank of the charge lattice is

$$R = (k-1)(nk-1), \quad (4.5)$$

which is equal to the rank of the quiver we just constructed. So we conjecture that the quiver from the network is the BPS quiver for the underlying field theory.

Example 2: Let's consider (A_2, A_2) theory, there are a total of 4 marked points on the boundary of the disc, and each marked point is labeled by a full puncture of A_2 group. The triangulation is very simple and the dot diagram in each triangle is easily found. The quiver has the shape of $A_2 \times A_2$, and confirm the result presented in [17]. The resulting quiver diagram is mutation equivalent to the D_4 Dynkin diagram, which is a further justification that the (A_2, A_2) theory is isomorphic to (A_1, D_4) theory as shown in figure. 12¹⁰. This isomorphism can also be checked from various other tests like the scaling spectrum, the central charges, three dimensional mirror, etc. The quiver for (A_3, A_3) theory is shown in figure. 13. If we first do quiver mutation on node 1 and 2, then do the quiver mutation on 3, the final quiver is of the shape of a product of A_3 and A_3 Dynkin diagram. The interested reader can check the quiver is mutation equivalent to a product of two Dynkin diagrams for the general cases.

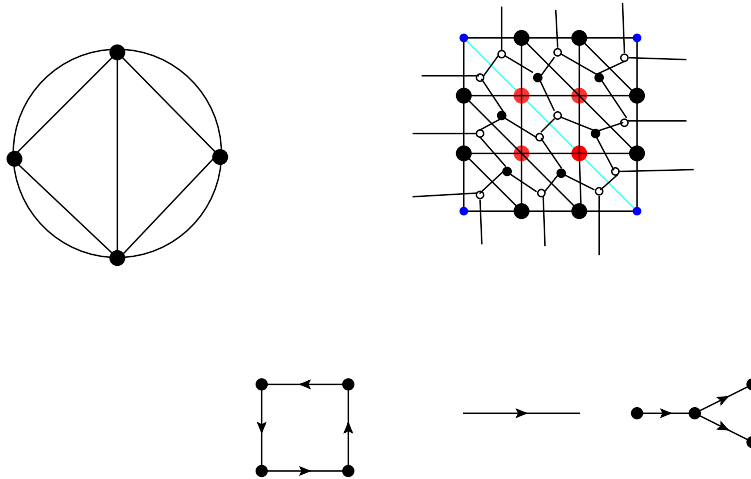


Figure 12: The network and the quiver for (A_2, A_2) theory. The quiver is mutation equivalent to D_4 Dynkin diagram.

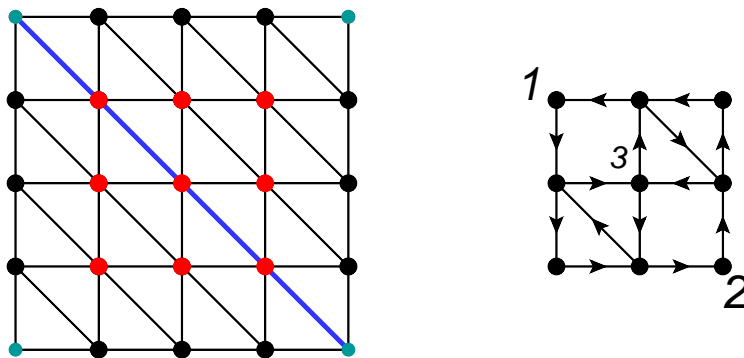


Figure 13: The tessellation for (A_3, A_3) theory and the quiver is mutation equivalent to A_3 times A_3 Dynkin diagram. This can be shown by first mutating nodes 1 and 2, then on node 3.

¹⁰We do not draw the network explicitly for most of the examples below.

After finding the network from the triangulation, one could find other quivers by doing square moves which are just the quiver mutation acting on the quivers. In particular, the network for different triangulations are related by a sequence of square moves.

Let's now find the invariant information associated with the network which is not changed under square move. One can find the permutations using zig-zag path which is invariant under the square move, and we do not have anything more to say about this. It is interesting to find the underlying Grassmannia though. The computation can be done by explicitly counting the degree of the various vertices.

First, there are a total of $(2n + 2)$ external edges and $(2n - 1)$ internal edges in the triangulation; There are a total of $2n$ triangles. The N of the network is easy to count: there are a total $(k - 1)(2n + 2)$ external edges in the network, so

$$N = (k - 1)(2n + 2). \quad (4.6)$$

Let's now count the degree of various vertices. There are $\frac{k(k-1)}{2}$ trivalent black vertices and $\frac{(k-3)(k-2)}{2}$ trivalent white vertices in each triangle. The white vertices on the boundary are a little bit complicated. The degree of white vertices on the internal edge is four, and the total number of such vertices are $(2n - 1)(k - 2)$; the white vertices on the external edge which is not living at the marked points has degree 3, and the total numbers are $(2n + 2)(k - 2)$. The white vertices at the marked points on the boundary can be counted using the special zig-zag triangulation, and there are two degree two vertices, two degree three vertices, and $(2n - 2)$ degree four vertices, so the total contribution of these white vertices are $2(2n - 1)$. Combining the above analysis, we have the following formula

$$K - ((k-1)(2n+2) - K) = 2n \left[\frac{k(k-1)}{2} - \frac{(k-3)(k-2)}{2} \right] - (2n+2)(k-2) - 2(2n-1)(k-2) - 2(2n-1), \quad (4.7)$$

we find $K = k$. So the corresponding Grassmannia is $G(2(n + 1)(k - 1), k)$.

4.1.3 Generic case

Let's now consider general (A_k, A_{nk-1+j}) theory with $0 < j < k$. The Stokes matrices analysis suggests that there are j more marked points which are labeled by simple Young Tableaux. The number of marked points and their labels are

$$full : 2(n + 1); \quad simple : j \tag{4.8}$$

The full punctures are grouped together.

Example 2 : Consider (A_{k-1}, A_1) theory, here we have $n = 0$ and $j = 2$ and there are two full punctures and two simple punctures. The quiver can be found using the tessellation of the quadrilateral bounded by two full punctures and two simple punctures. The quiver has indeed the shape of A_{k-1} Dynkin diagram.

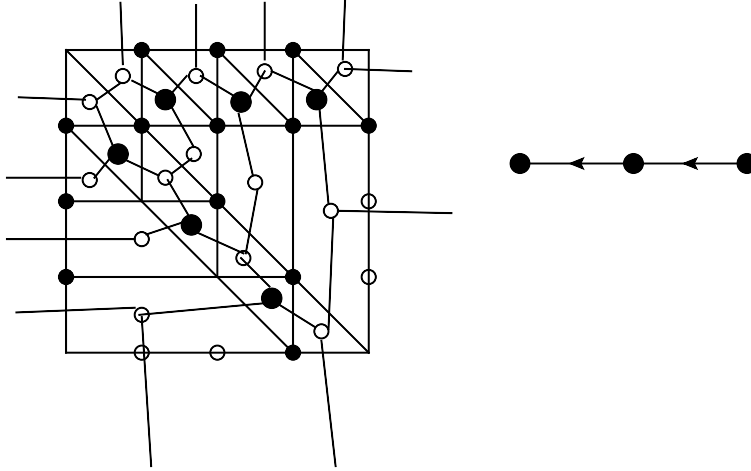


Figure 14: The network and the quiver for (A_3, A_1) theory. The quiver has the shape of A_3 Dynkin diagram.

Example 3: Consider (A_2, A_3) theory which is also isomorphic to (A_1, E_6) theory. This theory is engineered using A_2 theory with $n = 1$ and $j = 1$. There are four full punctures and one simple puncture according to our discussion of the Stokes phenomenon. The network and quiver are shown in figure. 15. The quiver from the network is not of the E_6 shape, but one can use the Java program [30] to show that it is mutation equivalent to E_6 Dynkin diagram ¹¹.

Example 4: This example deals with (A_2, A_4) theory which is expected to be isomorphic to (A_1, E_8) theory. There are four full punctures and two simple punctures on the boundary of the disc. The dot diagram and the quiver is shown in figure. 16. Using the Java program, it can be shown that the quiver is mutation equivalent to E_8 Dynkin diagram.

The network constructed is always a minimal network and we would also like to get some invariant information. The total external edges are $(2n + 2)(k - 1) + j$. We also find

¹¹First draw the quiver, and select tools and mutation class, you can find the simplest quiver in the mutation class.

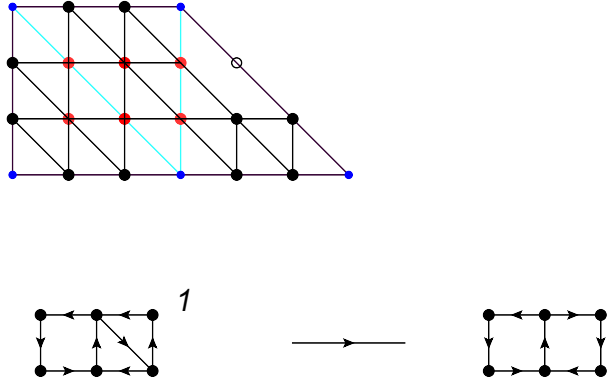


Figure 15: The tessellation and quiver for (A_2, A_3) theory, we have ignored the network and write the quiver directly. It is mutation equivalent to (A_2, A_3) quiver if we mutate the quiver node 1. One can also show that this quiver is mutation equivalent to E_6 Dynkin diagram.

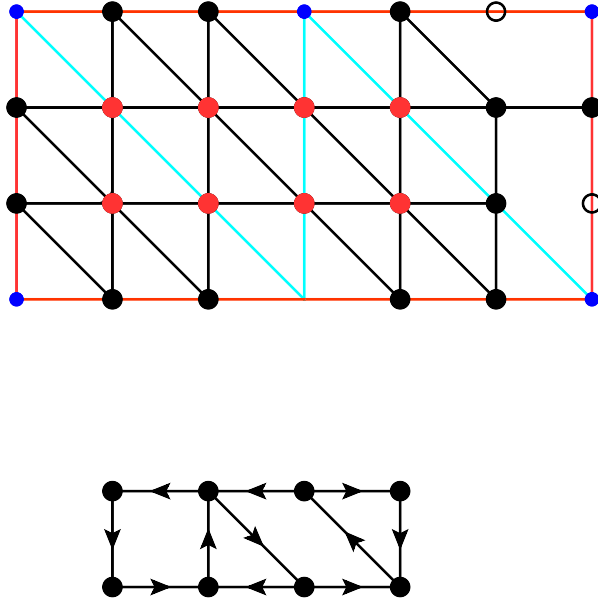


Figure 16: The tessellation and quiver for (A_2, A_4) theory; This quiver is not obviously mutation equivalent to quiver of A_2 Dynkin diagram times A_4 Dynkin diagram though. However, this quiver is mutation equivalent to E_8 Dynkin diagram by using the Java program, and E_8 quiver is also mutation equivalent to (A_2, A_4) theory.

that $K = k$ for many examples, so the corresponding Grassmannia is $G((2n+2)(k-1)+j, k)$. This seems to be the general result: the network from A_{k-1} theory on a disc always describe the Grassmannia $G(., k)$, it would be interesting to prove this fact.

If k is even and $j = k/2$, then there is another representation where we replace the j simple punctures with a full puncture. These two choice lead to two different quivers which are in the same mutation class. Let's also consider (A_3, A_1) theory, the two representations give the quivers in the same mutation class, see figure. 17. However, the networks for two representations are not in the same class, i.e. they are not related by square move .

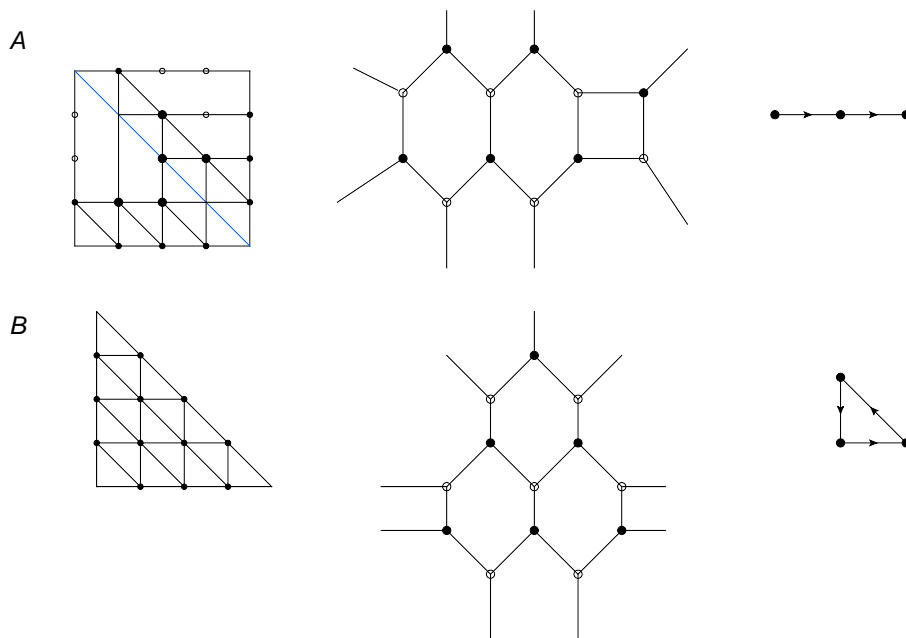


Figure 17: A: The network and quiver for (A_3, A_1) theory by using the simple punctures. B: The quiver derived using the full puncture. These two quivers are in the same mutation class.

Given the cyclic choices of the punctures, there are actually two ways of decorating the edges: clockwise or anti-clockwise [15]. However, in our current situation, they yield the same quiver mutation class. The idea is the following: consider the simple puncture and the triangulation where there are no internal edges ending on this puncture (this does not lose any generality since the quivers for different triangulations are related by the quiver mutations), then the effect of the special puncture is to cut a $(k - 1) \times (k - 1)$ triangle around this puncture, and this fact does not depend on how you choose to decorate the edges!

4.2 Type II AD theory

The type II AD theory is defined on a Riemann sphere with the following irregular singularity:

$$\Phi = \frac{A_r}{z^r} + \dots, \quad (4.9)$$

where $r = n + \frac{j}{k-1} + 2$ and A_r has the form

$$A_r = \text{diag}(0, 1, \omega, \dots, \omega^{k-2}), \quad (4.10)$$

with $\omega = \exp(\frac{2\pi i}{k-1})$. The total number of parameters from the Stokes matrix (equivalently total number of Stokes ray) is

$$N_{Stokes} = (n+1)k(k-1) + kj. \quad (4.11)$$

The total number of quiver nodes is the above number minus the dimension of the gauge group. Not surprisingly, the rank of the charge lattice of the corresponding AD theory has exactly same number by just counting the Coulomb branch and mass parameters. So we conjecture the quiver is the BPS quiver for the corresponding AD theory.

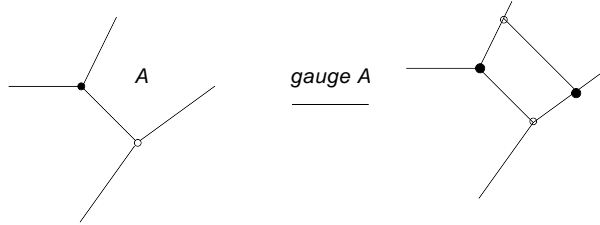


Figure 18: The open surface of the network is gauged by adding an extra edge.

The network is constructed from the triangulation of the disc with several marked points. There are $2(n+1)$ full punctures and j simple puncture. The boundary node of the simple puncture is going to be gauged. At the level of the network, we add an extra edge to close the open surface corresponding to the node on the simple puncture edge as shown in figure. 18¹². One interesting fact is that the network produced after this operation is still the minimal network and the Grassmannian cell is still of the form $G(\cdot, k)$.

Example 1: E_7 theory: The irregular singularity for this AD theory has $k = 3$ and $n = 1, j = 1$, there are 5 full punctures on the disc, the triangulation and the corresponding quiver is shown in figure. 19. The quiver from our construction is not as the form of E_7 Dynkin diagram, but after several quiver mutations, one can find that the quiver is indeed of the E_7 shape. There are other realizations in which we have four full punctures, and one simple puncture which are gauged. The dot diagram and the corresponding quiver is shown in figure. 19. The quiver is also mutation equivalent to the E_7 quiver by using the Java program.

Example 2: The irregular singularity of this theory has $n = 0, j = 2$ which is equivalent to (A_1, D_N) theory as shown in [3]. There are two full punctures and two simple

¹²This is like adding a BCFW bridge in the study of the scattering amplitude.

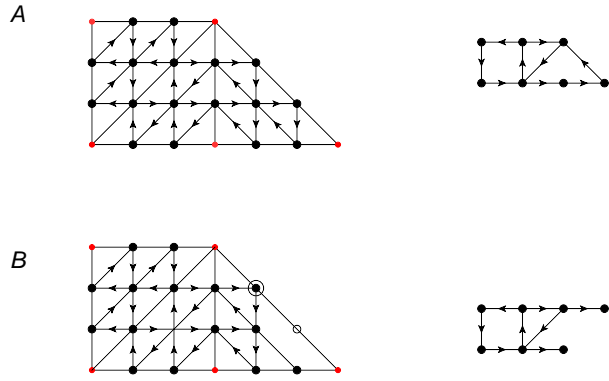


Figure 19: A: The triangulation of the disc of the E_7 theory using the full puncture representation. B: Another derivation using the gauging idea. One can show that these two quivers are mutation equivalent to each other using the Java program.

punctures which are going to be gauged. The resulting quiver is mutation equivalent to D_N Dynkin diagram which further confirms our previous identification.

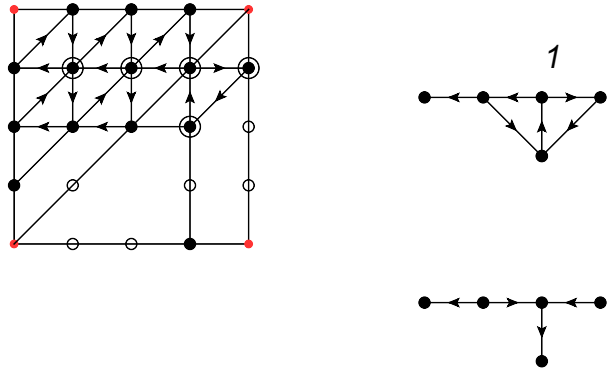


Figure 20: This type II network leads to D_N quiver.

4.3 Type III AD theory

This theory is specified by a sequence of Young Tableaux $Y_n \subset Y_{n-1} \dots \subset Y_1$. The charge lattice of the corresponding AD theory has dimension:

$$R = 2\left(\sum_{i=n}^{i=1} \dim(Y_i) - \dim(G)\right) + r, \quad (4.12)$$

where r is the number of heights of the Young Tableaux Y_1 .

The total number of Stokes rays are

$$N_{Stokes} = 2 \sum_{i=n}^{i=2} \dim(Y_i) \quad (4.13)$$

where $\dim(Y_i)$ is the dimension of the nilpotent orbit labeled by Young Tableaux Y_i . Now the disc model of this irregular singularity have twice number of Young Tableaux of Y_2 to Y_n , and the ideal triangulation will give the following number of quiver nodes

$$N_{nodes} = 2 \sum_{i=n}^{i=2} \dim(Y_i) - \dim(G). \quad (4.14)$$

We want this number to be the same as the dimension of the charge lattice of the field theory, and Y_1 should satisfy the following constraint:

$$2\dim(Y_1) + r = \dim(G), \quad (4.15)$$

which is only possible if Y_1 is a full Young Tableaux. This is the case we are going to discuss in this section.

Example 1: Let's take $Y_2 = [2, 3]$ and $Y_1 = [2, 1, 1, 1]$. Then the tessellation and the quiver is shown in figure. 21. The two networks are not minimal as discussed in [], this is one of the big difference with the network discussed in Grassamannia issue. It seems that the BPS quiver does not need the minimality condition, in fact, we are just care about the closed surface. There are two triangulations and the quiver is quiver mutation equivalent, although the underlying network is not square equivalent to each other, the quivers are mutation equivalent. According to the discussion in [3], this theory is isomorphic to the $SU(2)$ with four flavors whose BPS quiver is read from a sphere with four simple punctures of A_1 theory. The BPS quiver from that representation is shown in figure. 22, we can see that the rank 5 representation is indeed giving the same BPS quiver.

There is one question I would like to comment. According to the analysis presented in [15], the quiver from different triangulations are not related by the square move if the maximal height of the first Young Tableaux is bigger than one, and the minimal height of the next Young Tableaux in the cyclic order is also bigger than one. In our current example, the quivers from two triangulations are mutation equivalent if we only consider the internal nodes. We suspect this is true for all the triangulations and punctures.

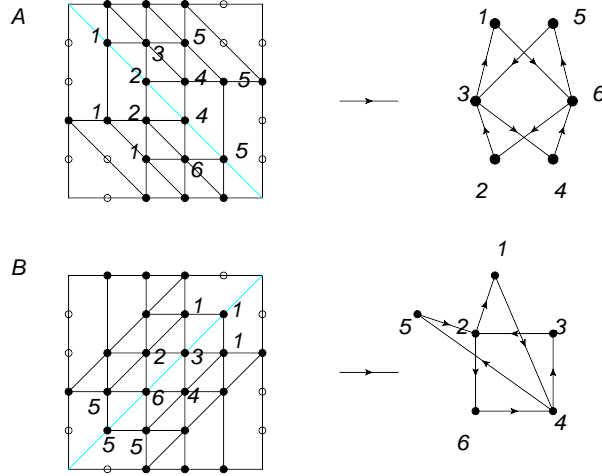


Figure 21: The triangulation and the quiver for a type III singularity with $Y_2 = [2, 3]$ and $Y_1 = [2, 1, 1, 1]$. The quiver is the same as the that of the $SU(2)$ with four flavors.



Figure 22: The quiver for $SU(2)$ with four flavors, which comes from the triangulation of the sphere with four full punctures of A_1 theory.

4.4 Type IV AD theory

One could add another regular puncture to above irregular puncture, then the corresponding Riemann surface is a disc with marked points and one bulk puncture. The triangulation of this Riemann surface can be easily found, the decoration of the external edge is the same as the previous case, and One of edge coming into the bulk puncture should be decorated using the Young Tableaux. The total number of quiver nodes from the Young Tableaux is the same as the charge lattice of the field theory. Let's work out some examples in detail.

Example 1: The (A_1, D_{N+2}) theory is engineered from six dimensional A_1 theory on a sphere with one irregular singularity and one regular singularity. The bordered Riemann surface is just a disc with several puncture and one bulk puncture. One triangulation and the quiver is shown in figure. 23 which is exactly of the D type Dynkin diagram shape and justifies the name of the theory. One could also write a planar network and the network is not minimal precisely because of the presence of the bulk puncture. The simple higher rank generalization is to replace each puncture with the full puncture. The triangulation is the same and each triangle has internal structures, the full quiver is straightforward to find. More generally, one could use any of the irregular singularity studied in previous subsection and find the corresponding BPS quiver pretty easily.

Example 2: This example is derived from using six dimensional A_2 theory, one has

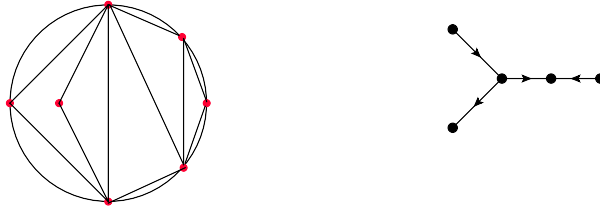


Figure 23: The triangulation and quiver for (A_1, D_{N+2}) theory.

two regular puncture on the boundary of the disc, and another full bulk puncture, the triangulation and the corresponding tessellation is given in figure.24. We find the quiver and it is the same as the $SU(2)$ with four flavors, which confirms the observation made in [3].

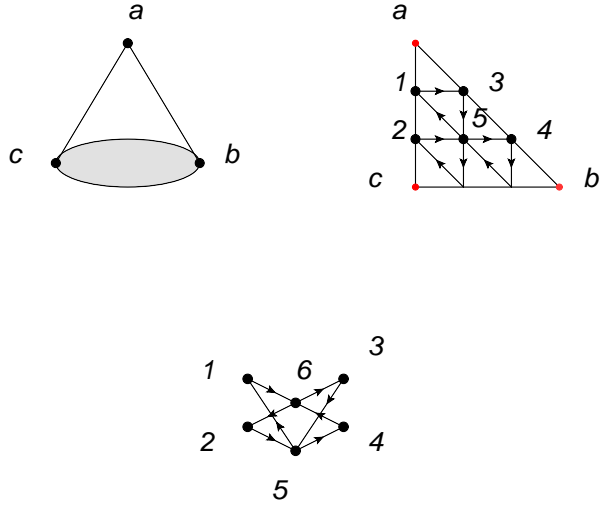


Figure 24: The triangulation of a disc with two full marked points and one full bulk puncture of $SU(3)$, the quiver is in the same mutation class of the $SU(2)$ with four flavors.

Example 3: Now let's consider A_3 theory and also two simple punctures on the boundary of the disc, and the bulk puncture is full. The triangulation and the quiver is given in figure. 25, it is remarkable that it is also the same as the $SU(2)$ with four flavors and this is a further justification of our claim made in [3].

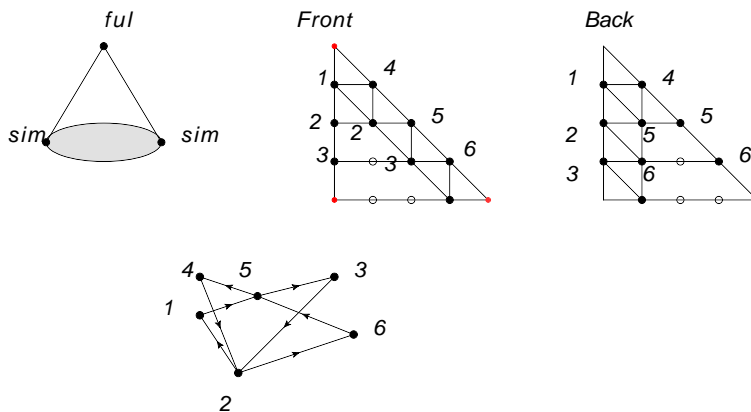


Figure 25: The quiver for a Type IV AD theory using A_4 theory which is actually isomorphic to $SU(2)$ with four flavors.

5. Cluster coordinates for asymptotical free theory

5.1 Linear quiver with Lagrangian descriptions

5.1.1 One gauge group

Let's first consider $SU(N)$ SQCD with various number of flavors. The six dimensional construction involves two irregular singularities which actually represent the number of flavors attached on the gauge group. The irregular singularity for n_f fundamental is [31]:

$$\Phi = \frac{1}{z^{1+\frac{1}{k-n_f}}} \text{diag}(0, \dots, 0, 1, \omega, \dots, \omega^{k-n_f-1}) + \frac{1}{z} \text{diag}(m_1, \dots, m_{n_f}, M, M, \dots, M). \quad (5.1)$$

Here $\omega = \exp(\frac{2\pi i}{k-n_f})$. When $n_f = k - 1$, one have a type III irregular singularity with Young Tableaux $Y_2 \subset Y_1$, here Y_2 is a simple and Y_1 is a full Young Tableaux.

The pure SYM case is rather simple, since there are two irregular singularities with the same type as the type I irregular singularity with $n = -1$ and $j = 1$. The Riemann surface is a annulus with one marked point on each boundary which is of the simple type. The triangulation of the annulus is presented in figure. 26: there are two triangles but the dot diagram is a little bit unclear from this perspective.

The triangulation can be best understood from the disc case using the following trick: one degenerate one of the hole and create two new marked points which are taken as the full puncture, then one use the familiar triangulations of fourth puncture disc to find the quiver and identify the boundary quiver nodes on the two edges representing the full puncture. The BPS quiver should include these identified boundary nodes. The quiver we find is exactly the same as found in the literature. The underlying network construction has several useful advantages, for example, we know we should mutate quiver nodes (1, 2, 3) together which correspond to the flip of the triangulation, the new quiver is isomorphic to the original quiver. Such quiver mutations are very important for finding the BPS spectrum. Moreover, the potential for this quiver is also manifest from the network construction.

The irregular singularity for $n_1 = 1$ is type II singularity with $n = -1$ and $j = 1$, and the boundary node for this simple puncture should be gauged. For generic n_f , the

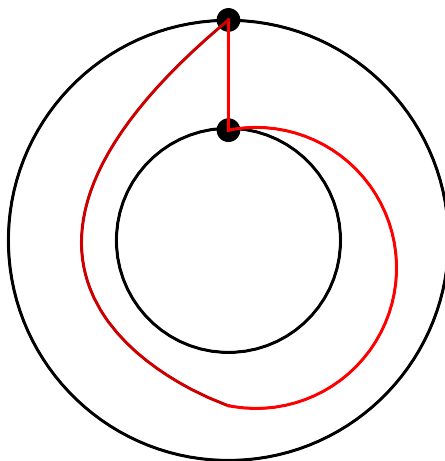


Figure 26: Triangulation of the annulus relevant for pure SYM theory.

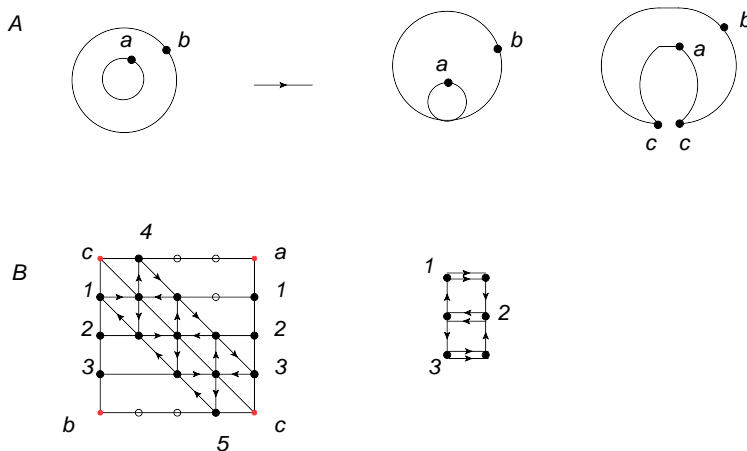


Figure 27: A: The degeneration limit of the annulus creates two new full punctures. The cyclic order for the four punctures are a, c, b, c , where a, b are the simple punctures and c is full puncture. B: We first construct the dot diagram, network(neglected) and the quiver for the four punctured disc. At the end, we need to identify the quiver nodes $(1, 2, 3)$. Finally we find the quiver for pure Super Yang-Mills theory.

number of Stokes rays are not enough to describe the moduli space. However, motivated by the above treatment of the $n_f = 1$, we conjecture that we get n_f extra nodes which are connected to the two nodes of pure $SU(N)$ by a cyclic triangle, see figure. 28 . This is in agreement with the result in [10].

If $n_1 = k - 1$, then the irregular singularity is the type III singularity and there are two simple punctures on the boundary. If $n_f = 0$ on the other boundary, the quiver is found by starting with a triangulation of the annulus with two simple punctures and one simple puncture on two boundaries respectively. The quiver is best understood from first decomposing the annulus into the disc, and there are two new full punctures which will be get identified in the end.

Notice that there are many choices for the triangulation given a decomposition of the

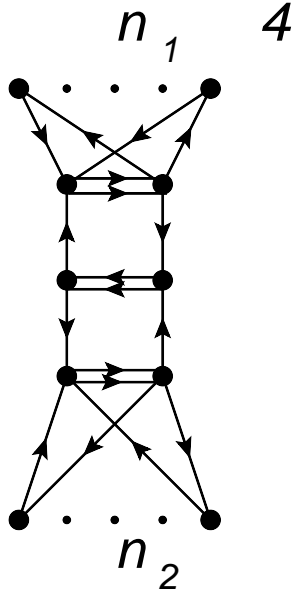


Figure 28: We add one more quiver node and a triangle of the quiver arrows to the boundary of the quiver of the pure Yang-Mills theory for each extra fundamentals.

number of flavors $n_f = n_1 + n_2$, and n_1, n_2 are the flavors represented by each boundary, it would be interesting to check that the quiver corresponding to difference choices are in the same mutation class. With this construction, we can find the quiver for $SU(k)$ gauge theory with any number of flavors $n_f < k$.

5.1.2 Linear quiver

Now let's consider the generic non-conformal quiver¹³ gauge theory. The simplest one is the following quiver $n_1 - SU(k) - \dots - SU(k) - n_2$, the six dimensional construction involves two irregular singularities describing n_1 and n_2 flavors for $SU(k)$, there are also several simple punctures in the bulk, the bordered Riemann surface for this theory is shown in figure. 29. The quiver is found by finding the triangulation and dot diagram of each triangle.

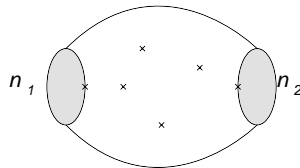


Figure 29: The bordered Riemann surface for the quiver gauge theory $n_1 - SU(k) - \dots - SU(k) - n_2$. All the punctures are the simple, and the special treatment is needed on the boundary simple puncture if $n_1, n_2 \geq 1$.

In general, we need to consider the quiver tail represented by the Young Tableaux with

¹³This quiver is the $\mathcal{N} = 2$ theory, which should not be confused with the BPS quiver.

rows r_1, r_2, \dots, r_s , and the quiver tail is

$$SU(h_1) - SU(h_2) - \dots - SU(h_s) \quad (5.2)$$

where $h_i = \sum_{j=1}^i r_j$ and $h_s = k$. The quiver tail we have studied above has a single row with length k . The general linear quiver which is UV complete has the following form

$$Tail_1 - SU(k) - SU(k) - \dots - SU(k) - Tail_2 \quad (5.3)$$

The irregular singularity for the quiver tail without any fundamentals has the following form

$$\Phi = \begin{pmatrix} B_1 & 0 & 0 & 0 & \dots \\ 0 & B_2 & 0 & 0 & \dots \\ 0 & 0 & B_3 & 0 & \dots \\ 0 & 0 & 0 & B_4 & \dots \\ \cdot & \cdot & \cdot & \cdot & \dots \end{pmatrix}$$

and $B_i = \frac{1}{1+r_i} \text{diag}(1, \omega, \dots, \omega^{r_i-1})$ with $\omega = \exp(\frac{2\pi i}{r_i})$. However, generally speaking the number of Stokes rays is not enough to describe the full framed moduli space. The special case is if $r_1 = r_2 = \dots = r_s$ and the irregular singularity is the type I singularity with $n = -1$ and $j = \frac{k}{r_s}$. There are j simple punctures on the boundary corresponding to this irregular singularity. After that, the quiver and the triangulation is straightforward to find.

Example: Consider the quiver $SU(2) - SU(4) - SU(6)$, and the Young Tableaux has rows 2, 2, 2. There are three simple punctures on one boundary and one simple puncture on the other boundary. The number of charge lattice of this theory is 20 which is the same as the quiver nodes from the triangulation of the bordered Riemann surface.

Another special case is the quiver tail

$$1 - SU(2) - SU(3) - \dots - SU(k) \quad (5.4)$$

the irregular singularity is a type I singularity with $n = 0$ and $j = 0$ and the leading order coefficient is regular semi-simple, so there are two full punctures on the boundary. The BPS quiver for the theory with this tail is then easy to find. It would be interesting to have other method to find the BPS quiver of general quiver tail.

5.2 Theory with AD matter

Now let's consider the asymptotical free theory defined by a Riemann surface with arbitrary number of irregular and regular singularities. The $\mathcal{N} = 2$ theory is a quiver gauge theory coupled with type IV AD theory and isolated theory represented by three regular singularities on a sphere.

To find the BPS quiver for this theory, one first blow up the irregular singularity into a disc with labeled marked points, and we have a bordered Riemann surface. Then we can find the triangulations, network and the quiver. For genus zero case, there is another construction coming from the disc: one first degenerate the boarded Riemann surface into

a disc, and there are two new full punctures¹⁴ appearing every time a hole is removed, and these new punctures are located at the boundary of the disc. Notice that there is a hidden cyclic order for all the punctures on the disc. The construction of the network of the disc with marked points is well understood, and finally we identify the quiver nodes associated with those punctures appearing from degenerating from the hole.

Example This theory has two irregular singularities which has integer order with leading order regular semi-simple, so the boarded Riemann surface model has two boundaries with full marked points. The gauge theory is a $SU(k)$ gauge group coupled with two Type IV theories which are realized as the Riemann sphere with one irregular singularity and one full regular singularity. The disc after the degeneration is shown in figure. 30,

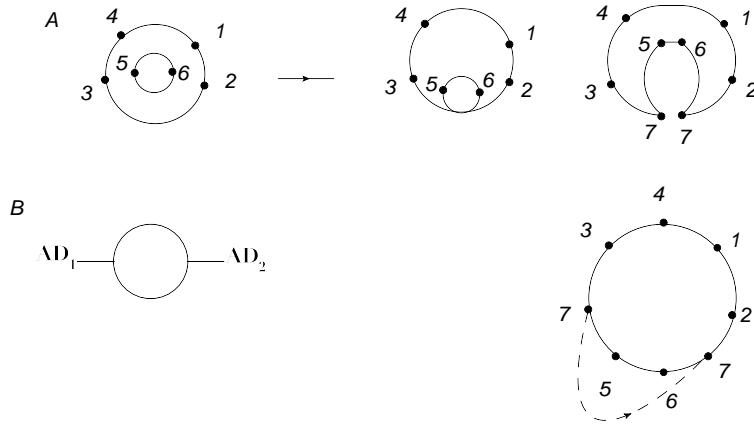


Figure 30: This is a $SU(k)$ theory coupled with two AD theories, all the marked points are full. The quiver can be found from the disc with marked points and then glue two punctures coming from the degeneration.

¹⁴This fact is similar to the theory of class \mathcal{S} in which two full punctures appear if a handle is removed, the difference is that there the punctures appear in the bulk of the Riemann surface.

6. Conclusion

We construct quiver and cluster coordinate for a large class of AD theory and asymptotical theory in this paper using the Stokes data for the irregular singularity. The planar network for type I or type II AD theory actually describes a positive cell in $G(., k)$ Grassmannia. The constructed network is automatically minimal and we hope our result could be useful for the study of the scattering amplitude in which such network plays a very important role [32]. These planar networks are also used in constructing four dimensional $\mathcal{N} = 1$ SCFT [33, 34] and our construction leads to so-called minimal duality frame. It is amazing that such simple combinatorial objects appear in so many completely different physical systems, it is definitely interesting to find the deep connections.

The quiver and quiver mutation are important in the study of the cluster coordinates. However, it is very hard to prove that two quivers are related by quiver mutations, especially if the quiver mutation class is infinite, which is the general case considered in this paper. The remarkable thing of the planar network is that one can actually define some quiver mutation invariant quantity using simple combinatorial tools. In fact, one can define a permutation [22] which uniquely fixed the network class related by square moves, therefore we can judge whether two quivers from networks are in the same mutation class. For our purpose, the network has some redundant information since we only care about the closed surface, so two quivers can be in the same mutation class even if the two networks are not in the same class. The permutation method is only a necessary condition but not the sufficient condition for the quiver mutation class. Moreover, there are networks defined on non-planar surface and no general method is known to judge whether two networks are related by square move. This question is deserved further study.

It would be interesting to compare our result with the spectral network construction proposed in [35], one possible clue is that the network can be equivalently replaced by a triple point diagram which seems to be closed related to some special configurations of spectral network.

We have not studied the cluster coordinates in any detail in this paper, such coordinates are important for studying the BPS spectrum and wall crossing behavior [36], in particular, quiver mutation sequences which lead back to original quiver can be easily found from our construction. Moreover, the network construction provides a very natural potential for the quiver, and the representation theory of quiver with potential could be used to study the spectrum and wall crossing. They are also very useful in studying the underlying hyperkahler metric of the Hitchin's moduli space [6, 37].

The line operator is related to the perfect matching of the network and one can define a boundary measurement using the cluster coordinates associated with the surfaces [22]. The boundary measurement is invariant under the square move which could be thought of as certain invariant information on crossing the wall, it is conceivable that these boundary measurements give the expectation value of the line operators. we believe many important physical information could be extracted from this fact, i.e. the framed BPS states counting.

A cluster integrable system [38] can be defined on the network which could be related to the Seiberg-Witten integrable system, and the quantization using cluster coordinates

is relatively easy. There is a very nice Poisson structure defined using the quiver and the quantization of the cluster coordinates should be related to the Nekrasov partition function. It is interesting to carry out this calculation in detail.

The cluster coordinate transformation for some special quiver mutations defines certain Y system [39], which is important for studying scattering amplitude and form factor of $\mathcal{N} = 4$ super Yang-mills theory in strongly coupling limit [40, 41]. We have explicitly constructed such Y system for a large class of cases, hopefully, this result could be useful in that context.

Acknowledgments

This research is supported in part by Zurich Financial services membership and by the U.S. Department of Energy, grant DE- FG02-90ER40542 (DX).

References

- [1] P. C. Argyres and M. R. Douglas, “New phenomena in SU(3) supersymmetric gauge theory,” *Nucl.Phys.* **B448** (1995) 93–126, [arXiv:hep-th/9505062](#) [hep-th].
- [2] P. C. Argyres, M. Plesser, and A. D. Shapere, “The Coulomb phase of N=2 supersymmetric QCD,” *Phys.Rev.Lett.* **75** (1995) 1699–1702, [arXiv:hep-th/9505100](#) [hep-th].
- [3] D. Xie, “General Argyres-Douglas Theory,” [arXiv:1204.2270](#) [hep-th].
- [4] O. Biquard and P. Boalch, “Wild non-abelian Hodge theory on curves,” *Compos. Math.* **140** (2004) no. 1, 179–204. <http://dx.doi.org/10.1112/S0010437X03000010>.
- [5] S. Fomin and A. Zelevinsky, “Cluster algebras I: Foundations,” *J. Amer. Math. Soc.* **15** (2002) 497–529, [arXiv:math/0104151](#).
- [6] D. Gaiotto, G. W. Moore, and A. Neitzke, “Four-dimensional wall-crossing via three-dimensional field theory,” *Commun.Math.Phys.* **299** (2010) 163–224, [arXiv:0807.4723](#) [hep-th].
- [7] D. Gaiotto, G. W. Moore, and A. Neitzke, “Wall-crossing, Hitchin Systems, and the WKB approximation,” [arXiv:0907.3987](#) [hep-th].
- [8] S. Cecotti and C. Vafa, “Classification of complete N=2 supersymmetric theories in 4 dimensions,” [arXiv:1103.5832](#) [hep-th].
- [9] M. Alim, S. Cecotti, C. Cordova, S. Espahbodi, A. Rastogi, and C. Vafa, “BPS Quivers and Spectra of Complete N=2 Quantum Field Theories,” [arXiv:1109.4941](#) [hep-th].
- [10] M. Alim, S. Cecotti, C. Cordova, S. Espahbodi, A. Rastogi, and C. Vafa, “N=2 Quantum Field Theories and Their BPS Quivers,” [arXiv:1112.3984](#) [hep-th].
- [11] N. Drukker, D. R. Morrison, and T. Okuda, “Loop operators and S-duality from curves on Riemann surfaces,” *JHEP* **0909** (2009) 031, [arXiv:0907.2593](#) [hep-th].
- [12] D. Gaiotto, G. W. Moore, and A. Neitzke, “Framed BPS states,” [arXiv:1006.0146](#) [hep-th].
- [13] D. Gaiotto, G. W. Moore, and A. Neitzke, “Wall-Crossing in Coupled 2d-4d Systems,” [arXiv:1103.2598](#) [hep-th].

- [14] E. Witten, “Gauge theory and wild ramification,” [arXiv:0710.0631 \[hep-th\]](#).
- [15] D. Xie, “Network, Cluster coordinates and N=2 theory I,” [arXiv:1203.4573 \[hep-th\]](#).
- [16] D. Gaiotto, “ $\mathcal{N} = 2$ dualities,” [arXiv:0904.2715 \[hep-th\]](#).
- [17] S. Cecotti, A. Neitzke, and C. Vafa, “R-twisting and 4d/2d correspondences,” [arXiv:1006.3435 \[hep-th\]](#).
- [18] S. Cecotti and M. Del Zotto, “On Arnold’s 14 ‘exceptional’ N=2 superconformal gauge theories,” *JHEP* **10** (2011) 099, [arXiv:1107.5747 \[hep-th\]](#).
- [19] M. Del Zotto, “More Arnold’s N = 2 superconformal gauge theories,” *JHEP* **11** (2011) 115, [arXiv:1110.3826 \[hep-th\]](#).
- [20] F. Benini, S. Benvenuti, and Y. Tachikawa, “Webs of five-Branes and $\mathcal{N} = 2$ superconformal field theories,” *JHEP* **09** (2009) 052, [arXiv:0906.0359 \[hep-th\]](#).
- [21] D. Nanopoulos and D. Xie, “ $N = 2$ generalized superconformal quiver gauge Theory,” [arXiv:1006.3486 \[hep-th\]](#).
- [22] A. Postnikov, “Total positivity, grassmannians, and networks,”. [arXiv.org:math/0609764](#).
- [23] V. V. Fock and A. B. Goncharov, “Moduli spaces of local systems and higher teichmuller theory,”. [arXiv.org:math/0311149](#).
- [24] A. Goncharov, “Ideal webs and moduli spaces of local systems on surfaces, to appear.”.
- [25] S. Fomin, M. Shapiro, and D. Thurston, “Cluster algebras and triangulated surfaces. part i: Cluster complexes,” *ACTA MATHEMATICA* **201** (2008) 83. [arXiv.org:math/0608367](#).
- [26] N. Hitchin, “The self-duality equation on a riemann surface,” *Proc.London Math.Soc.* **(3)55** (1987) 59–126.
- [27] A. Kapustin and E. Witten, “Electric-Magnetic duality and the Geometric Langlands Program,” [arXiv:hep-th/0604151](#).
- [28] W. Wasow, *Asymptotic expansions for ordinary differential equations*. Dover Publications Inc., New York, 1987. Reprint of the 1976 edition.
- [29] P. Boalch, “Geometry and braiding of stokes data; fission and wild character varieties,” 2011. <http://www.citebase.org/abstract?id=oai:arXiv.org:1107.0874>.
- [30] B. Keller, “Quiver mutation in Java,”. www.math.jussied.fr/~keller/quivermutation.
- [31] D. Nanopoulos and D. Xie, “Hitchin equation, irregular Singularity, and $N = 2$ asymptotical free theories,” [arXiv:1005.1350 \[hep-th\]](#).
- [32] N. Arkani-Hamed, J. L. Bourjaily, F. Cachazo, A. Goncharov, A. Postnikov, and J. Trnka, “Positive grassmannian and scattering amplitude,”. To appear.
- [33] D. Xie and M. Yamazaki, “Network and Seiberg Duality,” [arXiv:1207.0811 \[hep-th\]](#).
- [34] S. Franco, “Bipartite Field Theories: from D-Brane Probes to Scattering Amplitudes,” [arXiv:1207.0807 \[hep-th\]](#).
- [35] D. Gaiotto, G. W. Moore, and A. Neitzke, “Spectral networks,” [arXiv:1204.4824 \[hep-th\]](#).
- [36] D. Xie, “BPS spectrum, wall crossing and quantum dilogarithm identity, work in progress.”.
- [37] D. Xie, “3d $\mathcal{N} = 4$ field theory and Hyperkahler manifold, to appear.”.

- [38] A. B. Goncharov and R. Kenyon, “Dimers and cluster integrable systems,” [arXiv.org:1107.5588](https://arxiv.org/abs/1107.5588).
- [39] S. Fomin and N. Reading, “Y-systems and generalized associahedra,” *Ann. of Math* **158** 977–1018.
- [40] L. F. Alday, D. Gaiotto, and J. Maldacena, “Thermodynamic Bubble Ansatz,” *JHEP* **09** (2011) 032, [arXiv:0911.4708](https://arxiv.org/abs/0911.4708) [[hep-th](#)].
- [41] J. Maldacena and A. Zhiboedov, “Form factors at strong coupling via a Y-system,” *JHEP* **11** (2010) 104, [arXiv:1009.1139](https://arxiv.org/abs/1009.1139) [[hep-th](#)].